SEISMICA

When are Non-Double-Couple Components of Seismic Moment Tensors Reliable?

Boris Rösler [ID] * [1], **Seth Stein** [ID] [1,2], **Bruce D. Spencer** [ID] [2,3]

[1]Department of Earth and Planetary Sciences, Northwestern University, Evanston, Illinois, U.S.A., [2]Institute for Policy Research, Northwestern University, Evanston, Illinois, U.S.A., [3]Department of Statistics and Data Science, Northwestern University, Evanston, Illinois, U.S.A.

Abstract   There has been considerable discussion as to how to assess when non-double-couple (NDC) components of seismic moment tensors represent real source processes. We explore this question by comparing moment tensors (MTs) of earthquakes in three global catalogs, which use different inversion procedures. Their NDC components are only weakly correlated between catalogs, suggesting that they are largely artifacts of the inversion. A monotonic decrease in the NDC components' standard deviation with magnitude indicates increased reliability of the NDC components for larger earthquakes. The standard deviation begins to decrease for large NDC components exceeding 60%, suggesting that they represent real source processes. Randomly generated NDC components with the same mean and standard deviation as in the MT catalogs only reproduce some of this decrease. Thus NDC components of large earthquakes and NDC components that exceed 60% are likely to represent real source processes.

1   Introduction

Moment tensors provide a general description of seismic sources which may include components that differ from slip on planar faults, represented by double-couple (DC) force systems. Non-double-couple (NDC) components include isotropic components and compensated linear vector dipoles (CLVDs). CLVD components describe three force dipoles with one twice the magnitude of the others, yielding no volume change. Following the deployment of large digital seismic networks and the automatic derivation of moment tensors (MTs) after an earthquake, it was observed that many MTs had NDC components (Frohlich, 1994) whose geologic meaning has been debated (Sipkin, 1986; Miller et al., 1998).

Vavryčuk (2001, 2011) showed that the ratio of isotropic and CLVD components arising during the inversion depends on the ratio of the seismic velocities of P and S waves at the source. Thus, constraining the isotropic component also reduces the appearance of spurious CLVD components.

Additionally, the isotropic components of earthquake MTs are generally small (Kawakatsu, 1991; Okal et al., 2018). Therefore, catalogs usually constrain the isotropic component during the inversion to be zero and report only deviatoric MTs (Dziewonski and Woodhouse, 1983; Ekström et al., 2012). Because CLVD components are the only possible NDC components in deviatoric MT catalogs, we use the terms interchangeably.

Some earthquakes in specific geologic environments, notably volcanic ones, have NDC components that have been interpreted to represent real source processes (Kanamori and Given, 1982; Ross et al., 1996; Nettles and Ekström, 1998; Shuler et al., 2013a,b; Gudmundsson et al., 2016; Sandanbata et al., 2021; Rodríguez-Cardozo et al., 2021). Other NDC components reflect near-simultaneous rupture on nearby faults with different geometry (Hayes et al., 2010; Hamling et al., 2017; Scognamiglio et al., 2018; Yang et al., 2021; Ruhl et al., 2021) or a rupture with changes in geometry (Wald and Heaton, 1994; Cohee and Beroza, 1994; Pang et al., 2020). However, NDC components can also be artifacts of the MT inversion without geologic meaning (Ammon et al., 1994; Chapman, 2013).

Determining the origin of NDC components of earthquakes reported by MT inversions without additional information about the geologic setting of the earthquake is challenging. Rösler and Stein (2022) examined a large moment tensor dataset to assess how NDC components vary between earthquakes. Their general consistency with magnitude and faulting type and hence geologic environment suggests that most NDC components are artifacts of the inversion procedures used in compiling different catalogs.

However, several studies argue that there exists a threshold above which NDC components represent real source processes. Vavryčuk's 2002 study of $M < 3$ events in Bohemia placed this threshold between 20% and 40%. Stierle et al.'s 2014 analysis of $M < 4.1$ aftershocks of the 1999 Izmit earthquake found that spurious NDC components can reach 15%, and Adamová and Šílený's 2010 modeling study determined that spurious components can exceed 20%. In this study, we consider earthquakes worldwide with $4.4 \leq M_w \leq 8.6$ and use the differences between NDC components in different catalogs to assess their reliability and thus the issue of a possible threshold to derive criteria for the distinction between artifacts of the inversion and real source pro-

*Corresponding author: boris@earth.northwestern.edu

cesses.

2   Methodology

The Global CMT (GCMT) Project (Ekström et al., 2012), German Research Centre for Geosciences (GFZ), and U.S. Geological Survey (USGS, Hayes et al., 2009) catalogs report deviatoric moment tensors for a global distribution of earthquakes. We compile a dataset of 5000 earthquakes common to all three catalogs from July 2011 to December 2021 (Fig. 1), and identify MTs describing the same event by similar source times ($\pm 60\,$s), locations (difference less than $1°$), and magnitudes ($M_w \pm 0.5$). We use the USGS catalog's definition of the scalar moment as the Euclidean norm of the moment tensor (Silver and Jordan, 1982)

$$M_0 = \sqrt{\frac{1}{2} \sum_{i=1}^{3} \sum_{j=i}^{3} M_{ij}^2} \,, \tag{1}$$

where M_{ij} represent the six independent moment tensor components. This definition is equivalent to using the square root of the sums of the squares of the eigenvalues of the deviatoric moment tensor, λ'_i. This definition differs from that in the GCMT catalog, which uses the scalar moment of the best-fitting DC. From the scalar moment, we calculate the earthquake's moment magnitude following Kanamori (1977) as

$$M_w = \frac{2}{3} \left(\log_{10} M_0 - 9.1 \right) \,, \tag{2}$$

where M_0 is in $N \cdot m$.

Earthquakes common to all catalogs
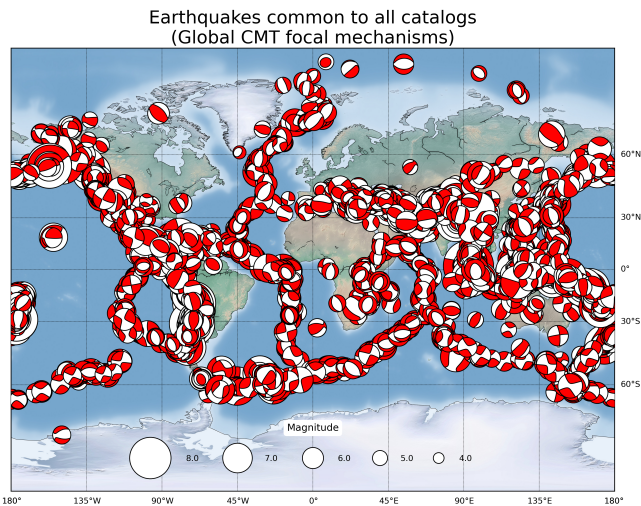(Global CMT focal mechanisms)

Figure 1 Location and focal mechanisms of the 5000 earthquakes used in this study. The earthquakes occurred between July 2011 and December 2021. Shown are the focal mechanisms in the Global CMT Project catalog.

For each earthquake, the NDC component in each catalog is obtained as the ratio of the absolutely smallest and absolutely largest eigenvalues of the MT (Giardini, 1984),

$$\epsilon = \frac{\lambda'_3}{\max(|\lambda'_1|, |\lambda'_2|)} \,, \tag{3}$$

where $\lambda'_1 > \lambda'_3 > \lambda'_2$ (Hudson et al., 1989). The NDC component is usually reported in moment tensor catalogs as 2ϵ with values from $-100\,\%$ to $100\,\%$ (Jost and Herrmann, 1989). The mean NDC component for an earthquake is calculated as the mean of the NDC components in the three catalogs

$$\bar{\epsilon} = \frac{1}{3} \sum_{i=1}^{3} \epsilon_i \,, \tag{4}$$

where the index i represents the three different catalogs. The NDC's standard deviation is

$$\sigma_{2\epsilon} = \sqrt{\frac{4}{3} \sum_{i=1}^{3} (\epsilon_i - \bar{\epsilon})^2} \,. \tag{5}$$

To classify earthquakes by faulting type, we calculate the plunge of the P-, N- (also called B-), and T-axes from the eigenvectors of the moment tensors (Frohlich, 1992). An earthquake is considered a normal faulting earthquake if the plunge of its P-axis satisfies $\sin^2 \delta_P \geq 2/3$ ($\delta_P \geq 54.75°$), strike-slip if its N-axis plunge exceeds $54.75°$, and a thrust fault if its T-axis plunge exceeds $54.75°$ (Saloor and Okal, 2018). If the plunge of none of the axes exceeds the threshold, we consider an earthquake to have oblique faulting.

3   Results

The NDC components in our dataset $2\overline{|\epsilon|}$ have a similar distribution with magnitude in all three catalogs (Fig. 2). The decrease with magnitude has been observed by Rösler and Stein (2022), who, using a large dataset compiled from multiple global and regional MT catalogs, found an average NDC component of $23.2\,\%$ that varies only slightly with magnitude.

However, the values of the NDC components 2ϵ for earthquakes in the three catalogs are only weakly correlated between catalogs (Fig. 3), consistent with findings by Frohlich and Davis (1999). The correlation coefficients vary between 0.49 for the NDC components reported in the GMCT and USGS catalogs, and 0.39 for the GFZ and USGS catalogs. Hence the standard deviation of the NDC components for each earthquake in the catalogs is a measure of the NDC component's consistency and can be used to assess the reliability of its determination. Fig. 4a shows that the standard deviation among the three catalogs $\sigma_{2\epsilon}$ decreases significantly with the magnitude of an earthquake, suggesting a more consistent determination of NDC components for larger earthquakes.

Rösler et al. (2021) found that the source processes of large earthquakes are more reliably determined, which is consistent with our dataset. Because the size of the NDC components varies only slightly for earthquakes of different magnitudes (Fig. 2), the decrease in their standard deviation cannot be due to their size, and we attribute it to the magnitude of the earthquakes. Thus, NDC components of large earthquakes are more reliably determined than the ones of small earthquakes, possibly due to moment tensor inversions for larger
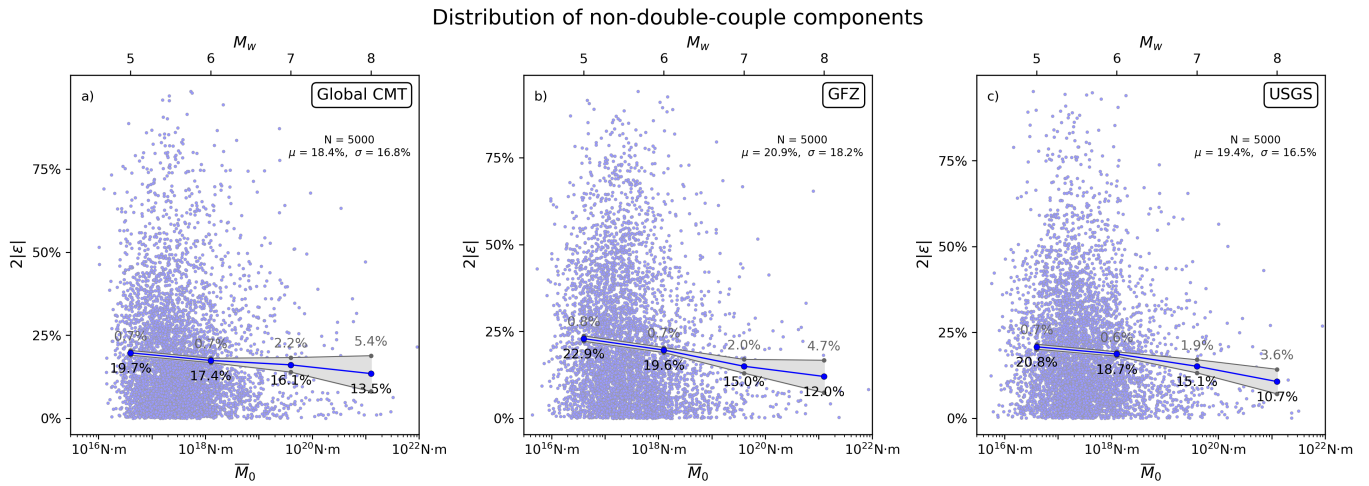
Distribution of non-double-couple components

Figure 2 Distribution of NDC components with magnitude in the three MT catalogs. Also shown are the mean NDC component and the $95\,\%$ confidence intervals, calculated as twice the standard deviation of the mean. The distribution in all catalogs is similar, with NDC components decreasing with magnitude.
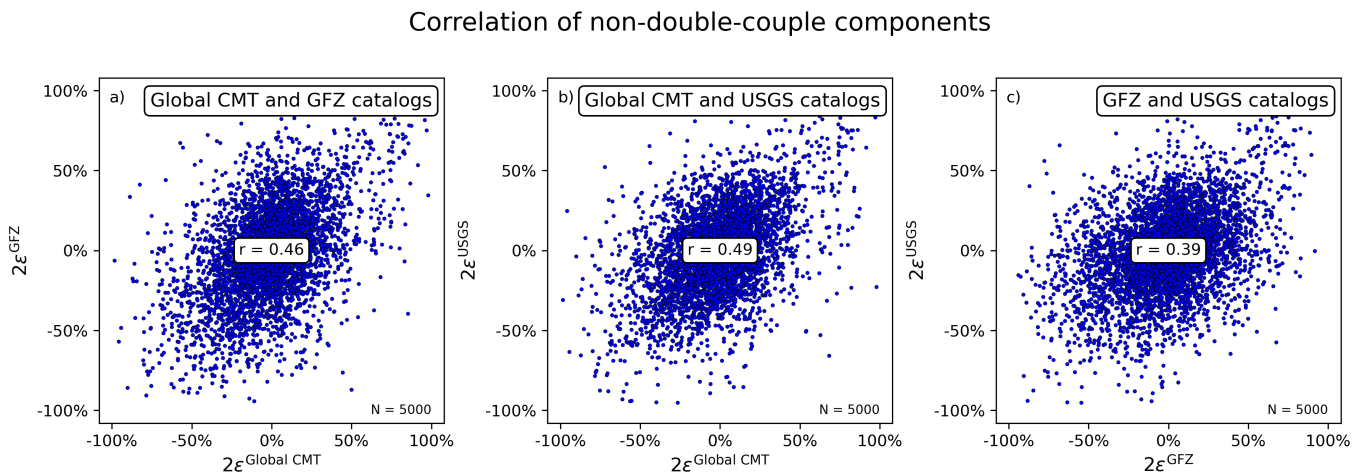
Correlation of non-double-couple components

Figure 3 Correlation of NDC components between each two of the three catalogs. Despite slight variations, the correlation between NDC components in different catalogs is weak, hinting at large uncertainties in their determination.

earthquakes being carried out using longer period seismic waves for which the velocity models agree better than for the shorter period seismic waves used for smaller earthquakes.

Similarly, Fig. 4b shows a decrease of the standard deviation for NDC components larger than $60\,\%$. This observation may support the existence of a threshold above which NDC components represent real source processes. However, a complexity arises for large NDC components because, by definition, these cannot exceed $100\,\%$. When the mean of the NDC components from the three catalogs is large in absolute value, the individual measurements tend to be closer than average. An extreme example illustrates this effect: If the NDC component has an average (among the three catalogs) of $99\,\%$, the largest variation that could occur among the three individual values is for $100\,\%$, $100\,\%$, and $97\,\%$, and for these values the standard deviation is below $1.75\,\%$. A related phenomenon is found in the binomial distribution in statistics, where the standard deviation decreases as the probability parameter increases beyond $50\,\%$.

To explore the possible impact of this ceiling effect, we conducted a simulation in which we randomly generated NDC components with the same mean as the observed triple from the three catalogs and the same standard deviation as the entire dataset. To do this, we first generated three sets of 5000 random values x, y, and z independently from a Gaussian distribution with zero mean and the standard deviation as in our dataset ($\sigma = 13.3\,\%$). We then set $X_i = \bar{\epsilon}_i + ax_i - by_i - bz_i$, $Y_i = \bar{\epsilon}_i - bx_i + ay_i - bz_i$, and $Z_i = \bar{\epsilon}_i - bx_i - by_i + az_i$ for all $i = 1, 2, \ldots, 5000$ with $a = (2/3)^{1/2}$, $b = (1/6)^{1/2}$, and $\bar{\epsilon}_i$ being the mean NDC component for each earthquake among the three catalogs. The resulting X, Y, and Z each have mean $\bar{\epsilon}_i$, standard deviation σ, and equal correlations so that the variance of their sum equals zero, i.e., $V(X+Y+Z) = 0$. The triples provide a set of three catalogs whose NDC components have the same mean and standard deviation as the observed datasets.

Fig. 5a shows that the standard deviation $\sigma_{2\epsilon}$ of these randomly generated NDC components does not vary with the size of the NDC components. However, this dataset contains values for which individual NDC com-
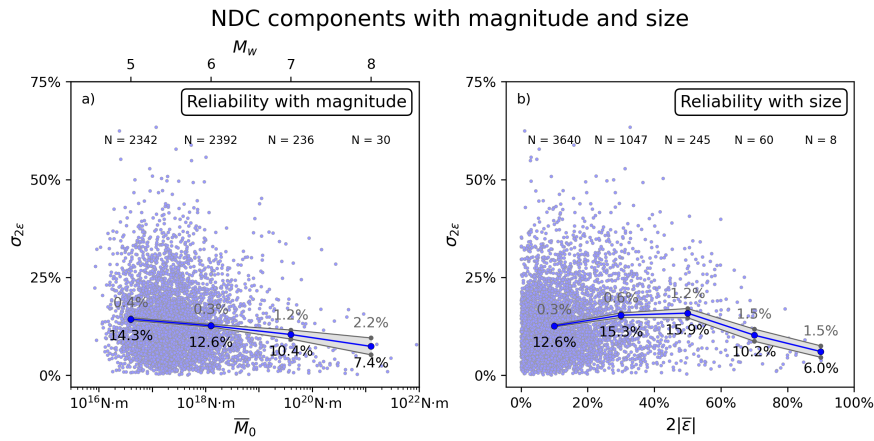
Figure 4 Standard deviation among NDC components in different catalogs with a) magnitude of the earthquake and b) size of the NDC component, and 95% confidence intervals for mean standard deviations. The standard deviation, a measure of their reproducibility, decreases significantly with magnitude, suggesting more reliable determination of NDC components for large earthquakes. The standard deviation decreases similarly for the largest NDC components.

ponents exceed $2|\epsilon| > 100\%$, which violates the definition of NDC components. Recall that the NDC component depends on the size of the absolutely smallest eigenvalue λ'_3. If λ'_3 becomes larger in absolute value than one of the other eigenvalues λ'_1 or λ'_2 where $2|\epsilon| > 100\%$, the eigenvalues switch order and the NDC component decreases in size and approaches a DC source again.

Discarding earthquakes for which individual NDC components X_i, Y_i, or Z_i exceed the ceiling of 100% truncates the random dataset to values which are physically possible. Because individual NDC components of $2|\epsilon| > 100\%$ are more likely for large mean NDC components, the bin of largest NDC components with $2|\epsilon| > 80\%$ is expected to be the most affected by this truncation. Fig. 5b shows that this process eliminates the triples of random NDC components with the largest standard deviation, leading to a decrease in standard deviation for the bin of largest NDC components while leaving other bins practically unchanged. This decrease is similar to that in the observed dataset (Fig. 4b). Repeating this experiment $10\,000$ times results in an average decrease in standard deviation of 3.3% for this bin (Fig. 5c), which is smaller than in the observed dataset. Instead of discarding earthquakes with NDC components larger than 100%, it is also possible to include them with smaller NDC components in this experiment. This can be done in different ways: if we limit the largest NDC components to 100%, we increase the smallest NDC component by the same amount by which the largest NDC component exceeded 100%, to preserve the mean of each triple. Repeating this experiment $10\,000$ times results in an average decrease in standard deviation of 2.0% in the largest size bin after modification of the NDC components exceeding 100%. Reducing the largest NDC components to values below 100% by an amount corresponding to which those NDC components exceeded 100% is equivalent to a decrease in NDC components when the smallest eigenvalue λ'_3 continues to increase and switches order with another eigenvalue. To preserve the mean of each triple of NDC components

in this case, we increase the smallest NDC component by twice the amount by which the largest NDC component exceeded 100%. Repeating this experiment $10\,000$ times results in a decrease in standard deviation of 3.1% for the bin of largest NDC components, comparable in size to discarding triples where individual values exceed values allowed by their definition, which resulted in a decrease of 3.3% in standard deviation. The standard deviation can be minimized when also modifying the intermediate NDC component: Assuming $|X_i| \geq |Y_i| \geq |Z_i|$, we calculate $d = \text{sgn}(X_i)(|X_i| - 100\%)$ and replace X_i by $X_i - 2d$, Y_i by $Y_i + gd$, and Z_i by $Z_i + (2 - g)d$, where $g = 1 - (Y_i - Z_i)/(2d)$. If the new value of Y_i exceeds 100%, we reduce it to 100% and increase X_i accordingly. In this case, the standard deviation decreases by 4.0% after $10\,000$ repetitions in the largest NDC components bin.

Therefore, this ceiling effect produces a distribution of standard deviation $\sigma_{2\epsilon}$ with size of the NDC component similar to that in the MT catalogs, but with a smaller decrease in the bin of largest NDC components. The observed dataset shows a standard deviation of 6.0% for NDC components larger than 80%, 7.3% smaller than the standard deviation for the complete dataset of 13.3%. Moreover, the ceiling effect does not reproduce the observed decrease in standard deviation for the bin of second largest NDC components between 60% and 80%, where the random NDC components only show an insignificant change. We hence conclude that the largest NDC components are, on average, more reliably determined. However, the threshold above which NDC components can be considered reliable, based on the significant decrease in standard deviation among NDC components in different catalogs lies at around 60%. This value is much larger than proposed in earlier studies.

Rösler and Stein (2022) noticed small differences in the size of NDC components of earthquakes with different faulting types. Consistent with their observation, thrust-faulting earthquakes have the smallest NDC components on average of all different faulting types
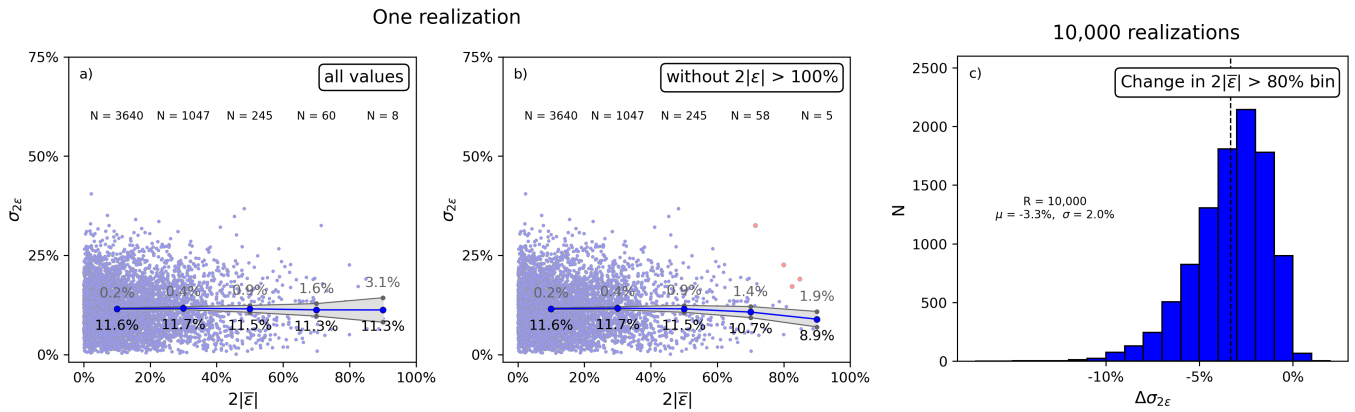
Figure 5 a) Standard deviation of randomly generated NDC components from a Gaussian distribution with the same mean and standard deviation as the MTs in our dataset. The standard deviation is constant over the range of sizes of NDC components. b) Some randomly generated NDC components exceed $100\,\%$ (marked in red). Discarding these values decreases the standard deviation for the largest NDC component bin ($2|\epsilon| > 80\,\%$). c) Repeating this experiment $10\,000$ times yields a $3.3\,\%$ average decrease, smaller than for the observed NDC components.

in our dataset (Fig. 6a). Their standard deviation $\sigma_{2\epsilon}$ between catalogs varies as well, with that for thrust-faulting earthquakes being the smallest (Fig. 6b). This is expected because the standard deviation of a Gaussian distribution with zero mean determines the mean of the absolute values. Therefore, it is unsurprising that the standard deviation of the different faulting types $\sigma_{2\epsilon}$ reflects the average size of NDC components $2|\epsilon|$, which suggests that the reliability between NDC components does not vary between faulting types.
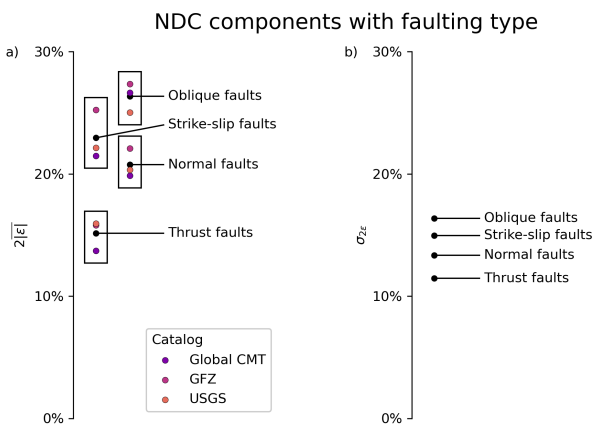

Figure 6 a) Mean NDC components of earthquakes with different faulting types in the three catalogs and their mean for each faulting type. The $95\,\%$ confidence interval is too small to be shown in the plot. b) Standard deviation of NDC components between catalogs for earthquakes with different faulting types. The standard deviation reflects the average size of the NDC components because the standard deviation of a Gaussian distribution with zero mean determines the mean of the absolute values. Therefore, the variation in standard deviation between faulting types does not reflect varying reliability.

4 Discussion and Conclusions

The moment tensors in global MT catalogs result from different inversion procedures. These procedures may vary in the stations used for the inversion, the individual weights given to the stations, the frequency of seismic waves analyzed, the processing of waveforms, and the inversion algorithm. Although the inversion results are also influenced by the Earth models used for the generation of Green's functions, the moment tensors in the three catalogs in this study were all calculated using Earth model PREM. The standard deviation between the NDC components in different catalogs is therefore a measure of their consistency and thus, presumably, their reliability. In this study, we use a dataset of 5000 MTs of earthquakes common to the catalogs of the Global CMT Project, the GFZ, and the USGS to assess the reliability of their NDC components.

The standard deviation of observed NDC components decreases for NDC components that are larger than $60\,\%$. Generating random NDC components with the same mean and standard deviation as the observed dataset shows that the decrease in standard deviation for the largest NDC components can be only partially explained by the constraint that NDC components must satisfy $2|\epsilon| < 100\,\%$ rather than a higher reliability of large NDC components. We therefore conclude that the largest NDC components are generally more reliably determined, and the threshold above which NDC components in global MT catalogs likely represent real source processes is about three times larger the observed average of NDC components of around $20\,\%$. Hence our sense is that an NDC component greater than $60\,\%$ is likely to reflect a real source process, although different moment tensor inversions may yield different results. Smaller NDC components are likely to be artifacts, and thus need further investigation before they can be considered real source processes.

The standard deviation between NDC components in different catalogs decreases monotonically with the
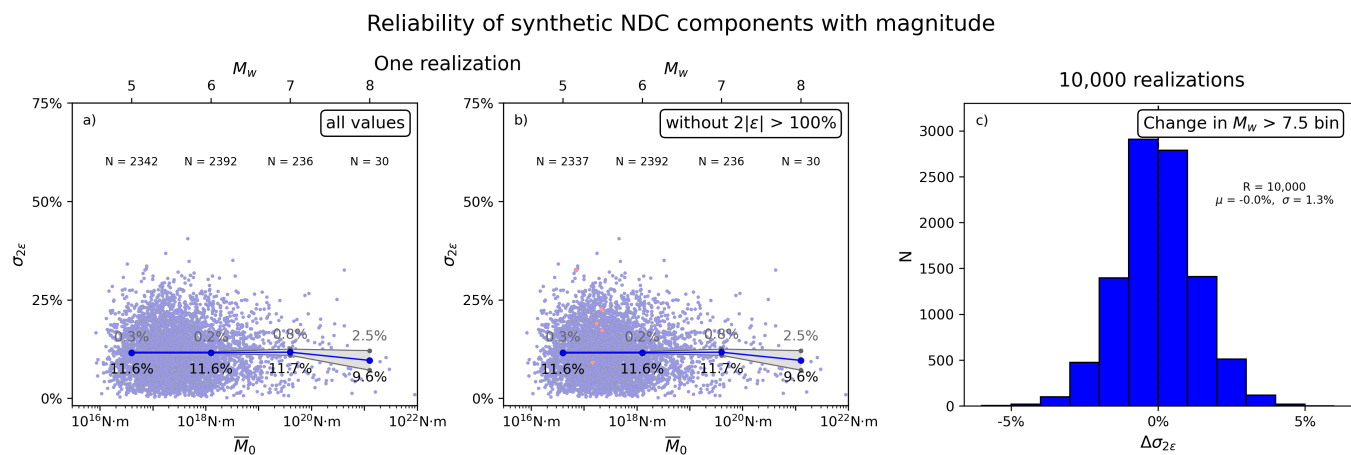
Figure 7 a) Standard deviation of the randomly generated NDC components in Fig. 3 with magnitude. The standard deviation is constant over all magnitudes. b) Discarding values for which individual NDC components exceed $2|\epsilon| > 100\%$ does not have influence on the standard deviation in any magnitude bin. c) Repeating this experiment $10\,000$ times shows that deleting large NDC components does not affect the standard deviation in the largest magnitude bin. Therefore, randomly generated NDC components cannot reproduce the observed decrease in standard deviation for the largest earthquakes, which suggests an increased reliability of NDC components for large earthquakes.

magnitude of an earthquake (Fig. 4a). Figs 7a and 7b show that the randomly generated NDC components exceeding 100% are distributed arbitrarily among the magnitude bins. They are most likely to fall into the magnitude bins with the most earthquakes and hence the smallest magnitude bins. In contrast to the distribution with size, the distribution of random NDC components with magnitude does not create a ceiling effect. Additionally, large earthquakes have, on average, smaller NDC components (Fig. 2). As a consequence, the largest magnitude bin is, in most cases, unaffected by NDC components exceeding a size of 100% and deleting them from the dataset or modifying them has no influence on the standard deviation in any magnitude bin. Repeating the experiment $10\,000$ times shows no difference in standard deviation in the largest magnitude bin. Therefore, in the absence of ceiling constraints, the observed decrease in standard deviation for NDC components of large earthquakes reflects the magnitude of an earthquake. As a consequence, the better agreement between catalogs suggests a higher reliability of NDC components of large earthquakes.

The variation of the NDC's standard deviation between faulting types does not reflect a variation in reliability, and is a consequence of the varying size of NDC components between faulting types. Therefore, only the variation of NDC components with earthquake magnitude and size appears to indicate at a variation in reliability of the NDC component.

Acknowledgements

We thank Emile Okal and Craig Bina for helpful discussions.

Data and code availability

The moment tensors used in this study were compiled from publicly available data sets. GCMT solutions

are from https://www.globalcmt.org (last accessed June 2022). The USGS and GFZ catalogs were downloaded using the Python package ObsPy (Beyreuther et al., 2010) and its International Federation of Digital Seismograph Networks webservice client (June 2022). A list of the earthquakes used in this study including their moment tensors in different catalogs is available by request from the authors.

Competing interests

The authors declare no competing interests.

References

Adamová, P. and Šílený, J. Non-double-couple earthquake mechanism as an artifact of the point-source approach applied to a finite-extent focus. *Bulletin of the Seismological Society of America*, 100(2):447–457, 2010. doi: 10.1785/0120090097.

Ammon, C. J., Lay, T., Velasco, A. A., and Vidale, J. E. Routine estimation of earthquake source complexity: The 18 October 1992 Colombian earthquake. *Bulletin of the Seismological Society of America*, 84(4):1266–1271, 1994. doi: 10.1785/B-SSA0840041266.

Beyreuther, M., Barsch, R., Krischer, L., Megies, T., Behr, Y., and Wassermann, J. ObsPy: A Python toolbox for seismology. *Seismological Research Letters*, 81(3):530–533, 2010. doi: 10.1785/gssrl.81.3.530.

Chapman, M. C. On the rupture process of the 23 August 2011 Virginia earthquake. *Bulletin of the Seismological Society of America*, 103(2A):613–628, 2013. doi: 10.1785/0120120229.

Cohee, B. P. and Beroza, G. C. Slip distribution of the 1992 Landers earthquake and its implications for earthquake source mechanics. *Bulletin of the Seismological Society of America*, 84(3): 692–712, 1994. doi: 10.1785/BSSA0840030692.

Dziewonski, A. M. and Woodhouse, J. An experiment in systematic study of global seismicity: centroid-moment tensor solutions for 201 moderate and large earthquakes of 1981. *Journal of Geophysical Research*, 88(B4):3247–3271, 1983. doi: 10.1029/JB088iB04p03247.

Ekström, G., Nettles, M., and Dziewonski, A. The global CMT project 2004-2010: Centroid-moment tensors for 13,017 earthquakes. *Physics of the Earth and Planetary Interiors*, 200-201:1–9, 2012. doi: 10.1016/j.pepi.2012.04.002.

Frohlich, C. Triangle diagrams: ternary graphs to display similarity and diversity of earthquake focal mechanisms. *Physics of the Earth and Planetary Interiors*, 75(1-3):193–198, 1992. doi: 10.1016/0031-9201(92)90130-N.

Frohlich, C. Earthquakes with non-double-couple mechanisms. *Science*, 264(5160):804–809, 1994. doi: 10.1126/science.264.5160.804.

Frohlich, C. and Davis, S. D. How well constrained are well-constrained T, B, and P axes in moment tensor catalogs? *Journal of Geophysical Research*, 104(B3):4901–4910, 1999. doi: 10.1029/1998JB900071.

Giardini, D. Systematic analysis of deep seismicity: 200 centroid-moment tensor solutions for earthquakes between 1977 and 1980. *Geophysical Journal International*, 77(3):883–914, 1984. doi: 10.1111/j.1365-246X.1984.tb02228.x.

Gudmundsson, M. T., Jónsdóttir, K., Hooper, A., Holohan, E. P., Halldórsson, S. A., Ófeigsson, B. G., Cesca, S., Vogfjörd, K. S., Sigmundsson, F., Högnadóttir, T., Einarsson, P., Sigmarsson, O., Jarosch, A. H., Jónasson, K., Magnússon, E., Hreinsdóttir, S., Bagnardi, M., Parks, M. M., Hjörleifsdóttir, V., Pálsson, F., Walter, T. R., Schöpfer, M. P. J., Heimann, S., Reynolds, H. I., Dumont, S., Bali, E., Gudfinnsson, G. H., Dahm, T., Roberts, M. J., Hensch, M., Belart, J. M. C., Spaans, K., Jakobsson, S., Gudmundsson, G. B., Fridriksdóttir, H. M., Drouin, V., Dürig, T., Aðalgeirsdóttir, G., Riishuus, M. S., Pedersen, G. B. M., Van Boeckel, T., Oddsson, B., Pfeffer, M. A., Barsotti, S., Bergsson, B., Donovan, A., Burton, M. R., and Aiuppa, A. Gradual caldera collapse at Bárðarbunga volcano, Iceland, regulated by lateral magma outflow. *Science*, 353(6296), 2016. doi: 10.1126/science.aaf8988.

Hamling, I. J., Hreinsdóttir, S., Clark, K., Elliott, J., Liang, C., Fielding, E., Litchfield, N., Villamor, P., Wallace, L., Wright, T. J., d'Anastasio, E., Bannister, S., Burbridge, D., Denys, P., Gentle, P., Howarth, J., Mueller, C., Palmer, N., Pearson, C., Power, W., Barnes, P., Barrell, D. J. A., van Dissen, R., Langridge, R., Little, T., Nicol, A., Pettinga, J., Rowland, J., and Stirling, M. Complex multifault rupture during the M_w 7.8 Kaikōura earthquake, New Zealand. *Science*, 356(6334), 2017. doi: 10.1126/science.aam7194.

Hayes, G. P., Rivera, L., and Kanamori, H. Source inversion of the W-Phase: real-time implementation and extension to low magnitudes. *Seismological Research Letters*, 80(5):817–822, 2009. doi: 10.1785/gssrl.80.5.817.

Hayes, G. P., Briggs, R. W., Sladen, A., Fielding, E. J., Prentice, C., Hudnut, K., Mann, P., Taylor, F. W., Crone, A. J., Gold, R., Ito, T., and Simons, M. Complex rupture during the 12 January 2010 Haiti earthquake. *Nature Geoscience*, 3(11):800–805, 2010. doi: 10.1038/ngeo977.

Hudson, J. A., Pearce, R. G., and Rogers, R. M. Source type plot for inversion of the moment tensor. *Journal of Geophysical Research: Solid Earth*, 94(B1):765–774, 1989. doi: 10.1029/JB094iB01p00765.

Jost, M. U. and Herrmann, R. B. A student's guide to and review of moment tensors. *Seismological Research Letters*, 60(2):37–57, 1989. doi: 10.1785/gssrl.60.2.37.

Kanamori, H. The energy release in great earthquakes. *Journal of Geophysical Research*, 82(20):2981–2987, 1977. doi: 10.1029/JB082i020p02981.

Kanamori, H. and Given, J. W. Analysis of long-period seismic waves excited by the May 18, 1980, eruption of Mount St. Helens - A terrestrial monopole? *Journal of Geophysical Research*, 87(B7):5422–5432, 1982. doi: 10.1029/JB087iB07p05422.

Kawakatsu, H. Insignificant isotropic component in the moment tensor of deep earthquakes. *Nature*, 351(6321):50–53, 1991. doi: 10.1038/351050a0.

Miller, A. D., Foulger, G. R., and Julian, B. R. Non-double-couple earthquakes 2. Observations. *Reviews of Geophysics*, 36(4): 551–568, 1998. doi: 10.1029/98RG00717.

Nettles, M. and Ekström, G. Faulting mechanism of anomalous earthquakes near Bárdarbunga Volcano, Iceland. *Journal of Geophysical Research: Solid Earth*, 103(B8):17973–17983, 1998. doi: 10.1029/98JB01392.

Okal, E. A., Saloor, N., Kirby, S. H., and Nettles, M. An implosive component to the source of the deep Sea of Okhotsk earthquake of 24 May 2013: Evidence from radial modes and CMT inversion. *Physics of the Earth and Planetary Interiors*, 281:68–78, 2018. doi: 10.1016/j.pepi.2017.10.006.

Pang, G., Koper, K. D., Mesimeri, M., Pankow, K. L., Baker, B., Farrell, J., Holt, J., Hale, J. M., Roberson, P., Burlacu, R., Pechmann, J. C., Whidden, K., Holt, M. M., Allamm, A., and DuRoss, C. Seismic analysis of the 2020 Magna, Utah, earthquake sequence: Evidence for a listric Wasatch fault. *Geophysical Research Letters*, 47(18), 2020. doi: 10.1029/2020GL089798.

Rodríguez-Cardozo, F., Hjörleifsdóttir, V., K., J., Iglesias, A., Franco, S. I., Geirsson, H., Trujillo-Castrillón, N., and M., H. The 2014-2015 complex collapse of the Bárðarbunga caldera, Iceland, revealed by seismic moment tensors. *Journal of Volcanology and Geothermal Research*, 416, 2021. doi: 10.1016/j.jvolgeores.2021.107275.

Rösler, B. and Stein, S. Consistency of Non-Double-Couple Components of Seismic Moment Tensors with Earthquake Magnitude and Mechanism. *Seismological Research Letters*, 93(3): 1510–1523, 2022. doi: 10.1785/0220210188.

Rösler, B., Stein, S., and Spencer, B. D. Uncertainties in Seismic Moment Tensors Inferred from Differences Between Global Catalogs. *Seismological Research Letters*, 92(6):3698–3711, 2021. doi: 10.1785/0220210066.

Ross, A., Foulger, G. R., and Julian, B. R. Non-double-couple earthquake mechanisms at the Geysers geothermal area, California. *Geophysical Research Letters*, 23(8):877–880, 1996. doi: 10.1029/96GL00590.

Ruhl, C. J., Morton, E. A., Bormann, J. M., Hatch-Ibarra, R., Ichinose, G., and Smith, K. D. Complex Fault Geometry of the 2020 M_{ww} 6.5 Monte Cristo Range, Nevada, Earthquake Sequence. *Seismological Research Letters*, 92(3):1876–1890, 2021. doi: 10.1785/0220200345.

Saloor, N. and Okal, E. A. Extension of the energy-to-moment parameter Θ to intermediate and deep earthquakes. *Physics of the Earth and Planetary Interiors*, 274:37–48, 2018. doi: 10.1016/j.pepi.2017.10.006.

Sandanbata, O., Kanamori, H., Rivera, L., Zhan, Z., Watada, S., and Satake, K. Moment tensors of ring-faulting at active volcanoes: Insights into vertical-CLVD earthquakes at the Sierra Negra caldera, Galápagos Islands. *Journal of Geophysical Research: Solid Earth*, 126(6), 2021. doi: 10.1029/2021JB021693.

Scognamiglio, L., Tinti, E., Casarotti, E., Pucci, S., Villani, F., Cocco, M., Magnoni, F., Michelini, A., and Dreger, D. Complex fault geometry and rupture dynamics of the M_w 6.5, 30 October 2016, Central Italy earthquake. *Journal of Geophysical Research*, 123 (4):2943–2964, 2018. doi: 10.1002/2018JB015603.

Shuler, A., Ekström, G., and Nettles, M. Physical mechanisms for vertical-CLVD earthquakes at active volcanoes. *Journal of Geophysical Research: Solid Earth*, 118(4):1569–1586, 2013a. doi: 10.1002/jgrb.50131.

Shuler, A., Nettles, M., and Ekström, G.   Global observation of vertical-CLVD earthquakes at active volcanoes. *Journal of Geophysical Research: Solid Earth*, 118(1):138–164, 2013b.   doi: 10.1029/2012JB009721.

Silver, P. G. and Jordan, T. H.   Optimal estimation of scalar seismic moment. *Geophysical Journal International*, 70(3):755–787, 1982. doi: 10.1111/j.1365-246X.1982.tb05982.x.

Sipkin, S. A.   Interpretation of non-double-couple earthquake mechanisms derived from moment tensor inversion.   *Journal of Geophysical Research: Solid Earth*, 91(B1):531–547, 1986. doi: 10.1029/JB091iB01p00531.

Stierle, E., Bohnhoff, M., and Vavryčuk, V.   Resolution of non-double-couple components in the seismic moment tensor using regional networks - II: application to aftershocks of the 1999 M_w 7.4 Izmit earthquake.   *Journal of Geophysical Research: Solid Earth*, 196(3):1878–1888, 2014. doi: 10.1093/gji/ggt503.

Vavryčuk, V. Inversion for parameters of tensile earthquakes. *Journal of Geophysical Research: Solid Earth*, 106(B8):16339–16355, 2001. doi: 10.1029/2001JB000372.

Vavryčuk, V.   Non-double-couple earthquakes of 1997 January in West Bohemia, Czech Republic: evidence of tensile faulting. *Geophysical Journal International*, 149(2):364–373, 2002.   doi: 10.1046/j.1365-246X.2002.01654.x.

Vavryčuk, V.   Tensile earthquakes: theory, modeling, and inversion.   *Journal of Geophysical Research: Solid Earth*, 116(B12), 2011. doi: 10.1029/2011JB008770.

Wald, D. J. and Heaton, T. H.   Spatial and temporal distribution of slip for the 1992 Landers, California, earthquake. *Bulletin of the Seismological Society of America*, 84(3):668–691, 1994.   doi: 10.1785/BSSA0840030668.

Yang, J., Zhu, H., Lay, T., Niu, Y., Ye, L., Lu, Z., Luo, B., Kanamori, H., Huang, J., and Li, Z.   Multi-fault opposing-dip strike-slip and normal-fault rupture during the 2020 M_w 6.5 Stanley, Idaho earthquake.   *Geophysical Research Letters*, 48(10), 2021.   doi: 10.1029/2021GL092510.